

FERMILAB-PUB-97/263-T
 NUHEP-TH-97-09
 AMES-HET-97-08
 July 1997

Single top quark production as a probe of R-parity-violating SUSY at pp and $p\bar{p}$ colliders

Robert J. Oakes^a, K. Whisnant^b, Jin Min Yang^{a,b,1}, Bing-Lin Young^b, and X. Zhang^{c,d}

^a *Department of Physics and Astronomy, Northwestern University,
 Evanston, Illinois 60208, USA*

^b *Department of Physics and Astronomy, Iowa State University,
 Ames, Iowa 50011, USA*

^c *Institute of High Energy Physics, Academia Sinica,
 Beijing 100039, China*

^d *Fermi National Accelerator Laboratory, P.O. Box 500, Batavia, IL 60510, USA*

ABSTRACT

We investigate the ability of single top quark production via $qq' \rightarrow$ squark $\rightarrow tb$ and $q\bar{q}' \rightarrow$ slepton $\rightarrow t\bar{b}$ at the LHC and Tevatron to probe the strength of R-parity violating couplings in the minimal supersymmetric model. We found that given the existing bounds on R-parity violating couplings, single top quark production may be greatly enhanced over that predicted by the standard model, and that both colliders can either discover R-parity violating SUSY or set strong constraints on the relevant R-parity violating couplings. We further found that the LHC is much more powerful than the Tevatron in probing the squark couplings, but the two colliders have comparable sensitivity for the slepton couplings.

PACS: 14.65.Ha, 14.80.Ly

¹On leave from Physics Department, Henan Normal University, China

1. Introduction

The HERA data showed excess events in deep-inelastic positron-proton scattering at high- Q^2 and high x , which are in apparent conflict with the Standard Model expectation [1]. The excess events have been interpreted as evidence of R-parity breaking supersymmetry[2]. Hence detailed examination of effects of R-parity breaking supersymmetry in other processes is in order. Some of the phenomenological implications of R-parity violating couplings at e^+e^- colliders have been investigated in Ref.[3]. Constraints on the R-parity violating couplings have also been obtained from perturbative unitarity [4,5], $n - \bar{n}$ oscillation [5,6], ν_e -Majorana mass [7], neutrino-less double β decay [8], charged current universality [9], $e - \mu - \tau$ universality [9], $\nu_\mu - e$ scattering [9], atomic parity violation [9], ν_μ deep-inelastic scattering [9], double nucleon decay [10], K decay [11,12], τ decay [13], D decay [13], B decay [14-16] and Z decay at LEPI [17,18]. Another important effect of R-parity violating couplings is that they may enhance the flavor changing top quark decays to the observable level of the upgraded Tevatron and LHC [19].

As is shown in Refs.[20-24], single top quark production is very interesting to study at the Tevatron and the LHC since, in contrast to the QCD process of $t\bar{t}$ pair production, it can be used to probe the electroweak theory. Single top production processes have been used to study the new physics effects involving the third-family quarks in a model independent approach [25] and in specific models [26,27]. More recently, motivated by the evidence of R-parity breaking supersymmetry [28,29] from the anomalous events at HERA [1], single top quark production $q\bar{q}' \rightarrow t\bar{b}$ at the Tevatron induced by baryon-number violating (BV) couplings λ'' (via the exchange of a squark in the t -channel) and by lepton-number violating (LV) couplings λ' (via the exchange of a slepton in the s -channel) has been studied [30] in minimal supersymmetric model (MSSM). It was found [30] that the upgraded Tevatron can probe the relevant BV couplings efficiently, while the probe for the relevant LV couplings is very limited.

In addition to the process $q\bar{q}' \rightarrow t\bar{b}$ mentioned above, which can be effectively studied at the Tevatron, the R-parity BV coupling can lead to the reaction $q\bar{q}' \rightarrow tb$ via an s-channel squark contribution which is suppressed at the Tevatron. This process is suitable for study at the LHC

and it probes a different set of BV couplings. In this paper we make a detailed study of the s-channel BV effect. For completeness we study the effect at both the LHC and the upgraded Tevatron. We also study the s-channel slepton contribution to $q\bar{q}' \rightarrow t\bar{b}$ at the LHC which we compare to the result obtained for the upgraded Tevatron [30].

This paper is organized as follows. In Sec.2 we present the Lagrangian for R-parity violating couplings and squared matrix elements for the processes $q\bar{q}' \rightarrow \text{squark} \rightarrow tb$ and $q\bar{q}' \rightarrow \text{slepton} \rightarrow t\bar{b}$. In Sec.3 we evaluate the signal for these processes and the SM background, and give the probing potential of the LHC in comparison to the upgraded Tevatron.

2. tb and $t\bar{b}$ production in R-parity violating MSSM

2.1 Lagrangian of R-parity violating couplings

The R-parity violating part of the superpotential of the MSSM is given by

$$\mathcal{W}_R = \lambda_{ijk} L_i L_j E_k^c + \lambda'_{ijk} L_i Q_j D_k^c + \lambda''_{ijk} U_i^c D_j^c D_k^c + \mu_i L_i H_2. \quad (1)$$

Here $L_i(Q_i)$ and $E_i(U_i, D_i)$ are the left-handed lepton (quark) doublet and right-handed lepton (quark) singlet chiral superfields, i, j, k are generation indices, and c denotes charge conjugation. $H_{1,2}$ are the chiral superfields representing the two Higgs doublets. The λ and λ' couplings violate lepton-number conservation, while the λ'' couplings violate baryon-number conservation. The coefficient λ_{ijk} is antisymmetric in the first two indices and λ''_{ijk} is antisymmetric in the last two indices. In terms of the four-component Dirac notation, the Lagrangians for the λ' and λ'' couplings that affect single top production at the Tevatron and the LHC are given by

$$\begin{aligned} \mathcal{L}_{\lambda'} &= -\lambda'_{ijk} \left[\tilde{\nu}_L^i \bar{d}_R^k d_L^j + \tilde{d}_L^j \bar{d}_R^k \nu_L^i + (\tilde{d}_R^k)^* (\bar{\nu}_L^i)^c d_L^j \right. \\ &\quad \left. - \tilde{e}_L^i \bar{d}_R^k u_L^j - \tilde{u}_L^j \bar{d}_R^k e_L^i - (\tilde{d}_R^k)^* (\bar{e}_L^i)^c u_L^j \right] + h.c., \end{aligned} \quad (2)$$

$$\mathcal{L}_{\lambda''} = -\lambda''_{ijk} \left[\tilde{d}_R^k (\bar{u}_L^i)^c d_L^j + \tilde{d}_R^j (\bar{d}_L^k)^c u_L^i + \tilde{u}_R^i (\bar{d}_L^j)^c d_L^k \right] + h.c.. \quad (3)$$

The terms proportional to λ are not relevant to our present discussion and will not be considered here. Note that while it is theoretically possible to have both BV and LV terms in

the Lagrangian, the non-observation of proton decay imposes very stringent conditions on their simultaneous presence[31]. We, therefore, assume the existence of either LV couplings or BV couplings, and investigate their separate effects in single top quark production.

2.2 $qq' \rightarrow \text{squark} \rightarrow tb$

Production of tb via an s -channel diagram $u^i d^j \rightarrow \tilde{d}_R^k \rightarrow tb$ can be induced by the BV couplings λ'' . The matrix element squared is given by

$$\overline{\sum} |M_{\lambda''}^{ij}|^2 = \frac{32}{3} \left| \sum_k \frac{\lambda''_{ijk} \lambda''_{33k}}{\hat{s} - M_{\tilde{d}^k}^2 + iM_{\tilde{d}^k} \Gamma_{\tilde{d}_R^k}} \right|^2 (p_1 \cdot p_2) [p_3 \cdot p_4 - M_t(s_t \cdot p_4)], \quad (4)$$

where p_1 and p_2 denote the momenta of the incoming quarks u^i and d^j , p_3 and p_4 of the outgoing t and b quarks. The center-of-mass energy of the parton is given by \hat{s} and s_t denotes the spin of top quark which is given by

$$s_t = \frac{h}{M_t} (|\vec{p}_3|, E_t \hat{p}_3), \quad (5)$$

where $h = \pm 1$ denotes the two helicity states, and \hat{p}_3 is the unit three-vector in the momentum direction of top quark.

Neglecting the contribution of third-family sea quark in the initial states, we obtain

$$\overline{\sum} |M_{\lambda''}(ud \rightarrow tb)|^2 = \frac{32}{3} \frac{(\lambda''_{112} \lambda''_{332})^2}{(\hat{s} - M_{\tilde{s}}^2)^2 + (M_{\tilde{s}} \Gamma_{\tilde{s}_R})^2} (p_1 \cdot p_2) [p_3 \cdot p_4 - M_t(s_t \cdot p_4)], \quad (6)$$

$$\overline{\sum} |M_{\lambda''}(us \rightarrow tb)|^2 = \frac{32}{3} \frac{(\lambda''_{112} \lambda''_{331})^2}{(\hat{s} - M_{\tilde{d}}^2)^2 + (M_{\tilde{d}} \Gamma_{\tilde{d}_R})^2} (p_1 \cdot p_2) [p_3 \cdot p_4 - M_t(s_t \cdot p_4)], \quad (7)$$

$$\overline{\sum} |M_{\lambda''}(cd \rightarrow tb)|^2 = \frac{32}{3} \frac{(\lambda''_{212} \lambda''_{332})^2}{(\hat{s} - M_{\tilde{s}}^2)^2 + (M_{\tilde{s}} \Gamma_{\tilde{s}_R})^2} (p_1 \cdot p_2) [p_3 \cdot p_4 - M_t(s_t \cdot p_4)], \quad (8)$$

$$\overline{\sum} |M_{\lambda''}(cs \rightarrow tb)|^2 = \frac{32}{3} \frac{(\lambda''_{212} \lambda''_{331})^2}{(\hat{s} - M_{\tilde{d}}^2)^2 + (M_{\tilde{d}} \Gamma_{\tilde{d}_R})^2} (p_1 \cdot p_2) [p_3 \cdot p_4 - M_t(s_t \cdot p_4)]. \quad (9)$$

In the R-parity conserving MSSM, the down-type squark \tilde{d}_R^k can decay into charginos and neutralinos via the processes $\tilde{d}_R^k \rightarrow u^k + \tilde{\chi}_j^{\pm}$ ($j = 1, 2$) and $\tilde{d}_R^k \rightarrow d^k + \tilde{\chi}_j^0$ ($j = 1, 2, 3, 4$), where $\tilde{\chi}_j^{\pm}$ and $\tilde{\chi}_j^0$ represent a chargino and neutralino, respectively [32]. Of course, it can also decay into gluino plus quark if kinematically allowed. In the R-parity violating MSSM, the down-type squark \tilde{d}_R^k can also decay into quark pairs $\tilde{d}^k \rightarrow \bar{d}^j + \bar{u}^i$ via the λ'' couplings. Since some of

the relevant λ'' couplings may be quite large, the width of a heavy down-type squark \tilde{d}_R^k can be large even if we do not consider the decay involving the gluino. We found that within the allowed parameter space (λ'' , chargino and neutralino sector) its width $\Gamma_{\tilde{d}_R}$ can be as large as $M_{\tilde{d}_R}/3$.

2.3 $q\bar{q}' \rightarrow \text{slepton} \rightarrow t\bar{b}$

Production of $t\bar{b}$ via an s -channel slepton $u^i\bar{d}^j \rightarrow \tilde{e}_L^k \rightarrow t\bar{b}$ can be induced by the LV couplings λ' . The matrix element squared is given by

$$\sum |M_{\lambda'}^{ij}|^2 = \frac{1}{2} \frac{\left(\lambda'_{1ij}\lambda'_{133} + \lambda'_{2ij}\lambda'_{233} + \lambda'_{3ij}\lambda'_{333}\right)^2}{(\hat{s} - M_{\tilde{e}_L}^2)^2 + (M_{\tilde{e}_L}\Gamma_{\tilde{e}_L})^2} (p_1 \cdot p_2) [p_3 \cdot p_4 - M_t(s_t \cdot p_4)], \quad (10)$$

where we assumed mass degeneracy for sleptons of different flavors.

In the R-parity conserving MSSM, the charged sleptons \tilde{e}_L will decay into charginos and neutralinos via the processes $\tilde{e}_L \rightarrow \nu_e + \tilde{\chi}_j^+$ ($j = 1, 2$) and $\tilde{e}_L \rightarrow e + \tilde{\chi}_j^0$ ($j = 1, 2, 3, 4$) [32]. However, in the R-parity violating MSSM, the slepton can also decay into quark pairs via the λ' couplings $\tilde{e}_L^i \rightarrow \bar{u}_L^j + d_R^k$. Since the allowed λ' couplings are quite small, the dominant decays are the chargino and neutralino modes. The partial widths are given by

$$\Gamma(\tilde{e}_L \rightarrow \nu_e + \tilde{\chi}_j^+) = \frac{g^2}{16\pi M_{\tilde{e}}^3} |U_{j1}|^2 \left(M_{\tilde{e}}^2 - M_{\tilde{\chi}_j^+}^2\right)^2, \quad (11)$$

$$\Gamma(\tilde{e}_L \rightarrow e + \tilde{\chi}_j^0) = \frac{g^2}{8\pi M_{\tilde{e}}^3} \left|s_W N'_{j1} + \frac{1}{c_W} \left(\frac{1}{2} - s_W^2\right) N'_{j2}\right|^2 \left(M_{\tilde{e}}^2 - M_{\tilde{\chi}_j^0}^2\right)^2, \quad (12)$$

where $s_W \equiv \sin \theta_W$, $c_W \equiv \cos \theta_W$ and the masses of the lepton and down-type quarks are neglected. The masses of charginos and neutralinos, and the matrix elements U_{ij} and N'_{ij} which respectively diagonalize the mass matrix of chargino and neutralino, depend on the SUSY parameters M_2 , M_1 , μ , and $\tan \beta$ [29]. Here, M_2 and M_1 are the masses of gauginos corresponding to $SU(2)$ and $U(1)$, respectively, μ is the coefficient of the $H_1 H_2$ mixing term in the superpotential, and $\tan \beta = v_2/v_1$ is the ratio of the vacuum expectation values of the two Higgs doublets.

3. Numerical calculation and results

Due to the large QCD backgrounds at hadron colliders, it is very difficult, if not impossible, to search for the signal from the hadronic decays of the top quark. We therefore look for events with $t \rightarrow W^+b \rightarrow l^+\nu b$ ($l = e, \mu$). (We take into account of the fact that the top quark is polarized in hadronic production.) Thus, the signature of this process is an energetic charged lepton, missing E_T , and double b -quark jets. We assumed silicon vertex tagging of the b -quark jet with 50% efficiency and the probability of 0.4% for a light quark jet to be mis-identified as a b -jet [33].

Although the present events have the unique signal of same sign b -quarks, since the tagging can not distinguish a b -quark jet from \bar{b} -quark jet, there are many potential SM backgrounds [33]:

- (1) the Drell-Yan like process $q\bar{q}' \rightarrow W^* \rightarrow t\bar{b}$;
- (2) the quark-gluon process $qg \rightarrow q'\bar{t}\bar{b}$ with a W -boson as an intermediate state in either the t -channel or the s -channel of a subdiagram;
- (3) processes involving a b -quark in the initial state, $bq(\bar{q}) \rightarrow tq'(\bar{q}')$ and $gb \rightarrow tW$;
- (4) $Wb\bar{b}$;
- (5) Wjj ;
- (6) $t\bar{t} \rightarrow W^-W^+b\bar{b}$.

Background process (2) contains an extra quark jet and can only mimic our signal if the quark misses detection by going into the beam pipe. This can only happen when the light quark jet has the pseudorapidity greater than about 3 or the transverse momentum less than about 10 GeV. In our calculation of the W -gluon fusion process as a background, we impose $\eta(q') > 3$ and $p_T(q') < 10$ GeV for the light-quark jet. The $bq(\bar{q}) \rightarrow tq'(\bar{q}')$ background is greatly reduced by requiring double b -tagging. The process $gb \rightarrow tW$ can only imitate our signal if the W decays into two jets, where one jet is missed by the detector and the other is mis-identified as a b quark, which should be negligible. Since we required two b -jets to be present in the final state and assumed the probability for a light quark jet to be mis-identified as a b -jet is 0.4%,

the potentially large background process (5) from Wjj is reduced to an insignificant level. Also we required the reconstructed top quark mass $M(bW)$ to lie within the mass range

$$|M(bW) - m_t| < 30 \text{ GeV}, \quad (13)$$

which can also reduce the backgrounds $Wb\bar{b}$ and Wjj efficiently. Background process (6) can mimic our signal if both W 's decay leptonically and one charged lepton is not detected, which we assumed to occur if $\eta(l) > 3$ and $p_T(l) < 10 \text{ GeV}$.

To make a realistic estimate we also need to consider the detector acceptance. To simulate the detector acceptance, we made a series of cuts on the transverse momentum (p_T), the pseudo-rapidity (η), and the separation in the azimuthal angle-pseudo rapidity plane ($\Delta R = \sqrt{(\Delta\phi)^2 + (\Delta\eta)^2}$) between a jet and a lepton or between two jets. For the upgraded Tevatron, the cuts are chosen to be

$$p_T^l, p_T^b, p_T^{\text{miss}} \geq 20 \text{ GeV}, \quad (14)$$

$$\eta_b, \eta_l \leq 2.5, \quad (15)$$

$$\Delta R_{jj}, \Delta R_{jl} \geq 0.5. \quad (16)$$

For the LHC, the cuts are chosen to be

$$p_T^l \geq 20 \text{ GeV}, \quad (17)$$

$$p_T^b \geq 35 \text{ GeV}, \quad (18)$$

$$p_T^{\text{miss}} \geq 30 \text{ GeV}, \quad (19)$$

$$\eta_b, \eta_l \leq 3, \quad (20)$$

$$\Delta R_{jj}, \Delta R_{jl} \geq 0.4. \quad (21)$$

To make the analyses more realistic, we simulate the detector effects by assuming a Gaussian smearing from the energy of the final state particles, given by:

$$\Delta E/E = 30\%/\sqrt{E} \oplus 1\%, \text{ for leptons}, \quad (22)$$

$$= 80\%/\sqrt{E} \oplus 5\%, \text{ for hadrons}, \quad (23)$$

where \oplus indicates that the energy dependent and independent terms are added in quadrature and E is in GeV.

We calculated the $p\bar{p}$ (for the Tevatron) and pp (for the LHC) cross sections for the signal with the MRSA' structure functions [34]. We have also examined the effect of using the CTEQ3M [35] structure functions and found the difference between the two sets of structure functions to be small. We have explicitly calculated backgrounds (1) and (2), and for the others used the Wjj background analysis of Ref.[36]. The effect of the cuts is shown in Table 1. Also, in our numerical calculation, we assumed $M_t = 175$ GeV, $\sqrt{s} = 2$ TeV for the upgraded Tevatron and $\sqrt{s} = 14$ TeV for the LHC. The integrated luminosities for both colliders are assumed to be 10 fb^{-1} . Assuming Poisson statistics, the number of signal events required for discovery of a signal at the 95% confidence level is approximately:

$$\frac{S}{\sqrt{S+B}} \geq 3 , \quad (24)$$

where S (B) is the number of signal (background) events obtained by multiplying the signal (background) cross section by the luminosity (10 fb^{-1}) and the tagging efficiency for two b -jets (0.5×0.5).

With all the above assumptions, we now present the results for both processes.

3.1 The B-violating process of tb production

For the BV process of tb production, $qq' \rightarrow \text{squark} \rightarrow tb$, we neglect $ud \rightarrow \tilde{s} \rightarrow tb$ and $us \rightarrow \tilde{d} \rightarrow tb$ since $\lambda''_{112} < 10^{-6}$ [10]. For simplicity, we assume λ''_{332} and λ''_{331} do not coexist and hence evaluate $cd \rightarrow \tilde{s} \rightarrow tb$ and $cs \rightarrow \tilde{d} \rightarrow tb$ separately.

Assuming $\Gamma_{\tilde{s}} = M_{\tilde{s}}/5$, we obtain Fig. 1 which shows the value of $\lambda''_{212}\lambda''_{332}$ versus strange-squark mass for $cd \rightarrow \tilde{s} \rightarrow tb$ to be observable at 95% confidence level. The region above each curve is the corresponding observable region. The solid curve is for the LHC, the dotted curve is for the upgraded Tevatron and the dashed line is the perturbative unitarity bound [4,5]. Here we see that both the LHC and the upgraded Tevatron can efficiently probe the relevant couplings, and the LHC serves a more powerful probe than the upgraded Tevatron.

As was discussed in the above section, the width of a down-type squark depends on many

free parameters, which can vary in a large range. In order to show the sensitivity of the results to the width of strange-squark, we present in Fig.2 the value of $\lambda''_{212}\lambda''_{332}$ versus the ratio $\Gamma_{\tilde{s}}/M_{\tilde{s}}$ for $cd \rightarrow \tilde{s} \rightarrow tb$ to be observable at 95% confidence level. Here we assume $M_{\tilde{s}} = 300$ GeV. The region above each curve is the corresponding observable region. The solid curve is for the LHC and the dashed curve is for the upgraded Tevatron. We see from this figure that the value of $\lambda''_{212}\lambda''_{332}$ varies mildly as a function of $\Gamma_{\tilde{s}}/M_{\tilde{s}}$. Again it is shown in this figure that the LHC is more powerful than the upgraded Tevatron in probing the relevant couplings.

The value of $\lambda''_{212}\lambda''_{331}$ versus down-squark mass for $cs \rightarrow \tilde{d} \rightarrow tb$ to be observable at 95% confidence level is shown in Fig.3. The region above each curve is the corresponding observable region. The solid curve is for the LHC, the dotted curve is for the upgraded Tevatron and the dashed line is the perturbative unitarity bound. The behaviour of this figure is similar to Fig.1. But for equal squark mass the value of $\lambda''_{212}\lambda''_{331}$ in Fig.3 is higher than the value of $\lambda''_{212}\lambda''_{332}$ in Fig.1. This shows that the process $cs \rightarrow \tilde{d} \rightarrow tb$ cannot be probed as efficiently as $cd \rightarrow \tilde{s} \rightarrow tb$ because of the relative suppression of the strange quark structure function compared to the valence down quark.

3.2 L-violating process of $t\bar{b}$ production

For the LV process of $t\bar{b}$ production, $q\bar{q}' \rightarrow \text{slepton} \rightarrow t\bar{b}$, we only consider the dominant process $u\bar{d} \rightarrow \text{slepton} \rightarrow t\bar{b}$ and thus provide the results for $\lambda'_{111}\lambda'_{133} + \lambda'_{211}\lambda'_{233} + \lambda'_{311}\lambda'_{333}$. The previous study [30] of this process at the upgraded Tevatron has shown that within the allowed range of the relevant coupling constants, this process is observable only when the slepton mass lies in a specific narrow range. Here we will determine if the LHC can do better than the upgraded Tevatron.

As discussed in the above section, the allowed λ' couplings which induce a charged slepton to decay into quark pairs are quite small and thus the dominant decays of a charged slepton are the chargino and neutralino modes. So we only consider the chargino and neutralino modes for simplicity. Then the width of the charged slepton only depends on the SUSY parameters M_2 , M_1 , μ and $\tan\beta$. In our calculation we use the GUT relation $M_1 = \frac{5}{3} \frac{g'^2}{g^2} M_2 \approx \frac{1}{2} M_2$, and fix $M_2 = -\mu = 250$ GeV and $\tan\beta = 2$. We checked that in this case the chargino and neutralino

masses are above the present lower limits from LEP II[37].

Figure 4 shows the value of $\lambda'_{111}\lambda'_{133} + \lambda'_{211}\lambda'_{233} + \lambda'_{311}\lambda'_{333}$ versus the slepton mass for $u\bar{d} \rightarrow$ slepton $\rightarrow t\bar{b}$ to be observable at 95% confidence level. The region above each curve is the corresponding observable region. The solid curve is for the LHC, the dotted curve is for the upgraded Tevatron and the dashed line is the value obtained by considering the following bounds for squark mass of 100 GeV [7,11,17]

$$|\lambda'_{i11}| < 0.012, \quad (i = 1, 2, 3), \quad (25)$$

$$|\lambda'_{133}| < 0.001, \quad (26)$$

$$|\lambda'_{233}| < 0.16, \quad (27)$$

$$|\lambda'_{333}| < 0.26. \quad (28)$$

Figure 4 shows that below the present upper limit for the couplings the LHC cannot do much better than the upgraded Tevatron in further probing the couplings.

In summary, we have studied single top quark production via $qq' \rightarrow$ squark $\rightarrow tb$ and $q\bar{q}' \rightarrow$ slepton $\rightarrow t\bar{b}$ at the Tevatron and the LHC in the MSSM with R-parity violation. Our results show that from the measurement of single top production, the LHC can efficiently probe the relevant R-parity violating couplings.

Acknowledgements

We would like to thank M. Hosch for help in evaluating some of the backgrounds, and A. Datta and A. P. Heinson for helpful discussions. X.Z. would like to thank the Fermilab theory group for the hospitality during the final stage of this work.

This work was supported in part by the U.S. Department of Energy, Division of High Energy Physics, under Grant Nos. DE-FG02-91-ER4086 DE-FG02-94ER40817, and DE-FG02-92ER40730. XZ was also supported in part by National Natural Science Foundation of China and JMY acknowledges the partial support provided by the Henan Distinguished Young Scholars Fund.

References

- [1] H1 Collab., C. Adloff et al., DESY 97-024; Zeus Collab., J. Breitweg et al., DESY 97-025.
- [2] D. Choudhury and S. Raychaudhuri, hep-ph/9702392; G. Altarelli, J. Ellis, G. F. Giudice, S. Lola and M. L. Mangano, hep-ph/9703276; H. Dreiner and P. Morawitz, hep-ph/9703279; J. Kalinowski, R. Rückl, H. Spiesberger and P. M. Zerwas, hep-ph/9703288; K. S. Babu, C. Kolda, J. M. Russell and F. Wilczek hep-ph/9703299; T. Kon and T. Kobayashi, hep-ph/9704221; J. E. Kim and P. Ko, hep-ph/9706387; U. Mahanta and A. Ghosal, hep-ph/9706398. S. Lola, hep-ph/9706519; M. Guchait and D. P. Roy, hep-ph/9707275; T. Kon, T. Matsushita and T. Kobayashi, hep-ph/9707355; M. Carena, D. Choudhury, S. Raychaudhuri and C. E. M. Wagner, hep-ph/9707458.
- [3] J. Erler, J. L. Feng and N. Polonsky, Phys. Rev. Lett. 78, 3063 (1997); D. K. Ghosh, S. Raychaudhuri and K. Sridhar, hep-ph/9608352; D. Choudhury and S. Raychaudhuri, hep-ph/9702392.
- [4] B. Brahmachari and P. Roy, Phys. Rev. D50, 39 (1994).
- [5] J. L. Goity and M. Sher, Phys. Lett. B346, 69 (1995).
- [6] F. Zwirner, Phys. Lett. B132, 103 (1983).
- [7] S. Dimopoulos and L. J. Hall, Phys. Lett. B207, 210 (1987); R. M. Godbole, P. Roy and X. Tata, Nucl. Phys. B401, 67 (1993).
- [8] R. N. Mohapatra, Phys. Rev. D34, 3457 (1986); M. Hirsch, H. V. Klapdor-Kleingrothaus, S. G. Kovalenko, Phys. Rev. Lett. 75, 17 (1995); K. S. Babu and R. N. Mohapatra, Phys. Rev. Lett. 75, 2276 (1995).
- [9] V. Barger, G. F. Giudice and T. Han, Phys. Rev. D40, 2978 (1989).
- [10] J. L. Goity and M. Sher, Phys. Lett. B346, 69 (1995).

- [11] K. Agashe and M. Graesser, Phys. Rev. D54, 4445 (1996).
- [12] D. Choudhury and P. Roy, hep-ph/9603363.
- [13] G. Bhattacharyya and D. Choudhury, Mod. Phys. Lett. A10, 1699 (1995).
- [14] D. E. Kaplan, hep-ph/9703347.
- [15] J. Jang, J. K. Kim and J. S. Lee, hep-ph/9701283.
- [16] J. Jang, J. K. Kim and J. S. Lee, hep-ph/9704213.
- [17] G. Bhattacharyya, J. Ellis and K. Sridhar, Mod. Phys. Lett. A10, 1583 (1995).
- [18] G. Bhattacharyya, D. Choudhury and K. Sridhar, Phys. Lett. B355, 193 (1995).
- [19] J. M. Yang, B.-L. Young and X. Zhang, hep-ph/9705341.
- [20] S. Willenbrock and D. Dicus, Phys. Rev. D34, 155 (1986); S. Dawson and S. Willenbrock, Nucl. Phys. B284, 449 (1987); C.-P. Yuan, Phys. Rev. D41, 42 (1990); F. Anselmo, B. van Eijk and G. Bordes, Phys. Rev. D45, 2312 (1992); R. K. Ellis and S. Parke, Phys. Rev. D46, 3785 (1992); D. Carlson and C.-P. Yuan, Phys. Lett. B306, 386 (1993); G. Bordes and B. van Eijk, Nucl. Phys. B435, 23 (1995); A. Heinson, A. Belyaev and E. Boos, hep-ph/9509274.
- [21] S. Cortese and R. Petronzio, Phys. Lett. B306, 386 (1993).
- [22] T. Stelzer and S. Willenbrock, Phys. Lett. B357, 125 (1995).
- [23] A. P. Heinson, hep-ex/9605010.
- [24] M. Smith and S. Willenbrock, Phys. Rev. D54, 6696 (1996); S. Mrenna and C.-P. Yuan, hep-ph/9703224.
- [25] A. Datta and X. Zhang, Phys. Rev. D55, 2530 (1997); K. Whisnant, J. M. Yang, B.-L. Young and X. Zhang, Phys. Rev. D56, 467 (1997).
- [26] C. S. Li, R. J. Oakes and J. M. Yang, Phys. Rev. D55, 1672 (1997); Phys. Rev. D55, 5780 (1997); hep-ph/9706412; G.-R. Lu et al., hep-ph/9701406
- [27] E. H. Simmons, hep-ph/9612402; C.-X. Yue, Y.-P. Kuang and G.-R. Lu, Phys. Rev. D56, 291 (1997).

- [28] For reviews of the MSSM, see, for example, H. E. Haber and G. L. Kane, Phys. Rep. 117, 75 (1985); J. F. Gunion and H. E. Haber, Nucl. Phys. B272, 1 (1986).
- [29] For reviews of R-parity violation, see, for example, G. Bhattacharyya, Nucl. Phys. Proc. Suppl. 52A, 83 (1997).
- [30] A. Datta, J. M. Yang, B.-L. Young and X. Zhang, hep-ph/9704257, to appear in Phys. Rev. D.
- [31] C. Carlson, P. Roy and M. Sher, Phys. Lett. B357, 99 (1995); A. Y. Smirnov and F. Vissani, Phys. Lett. B380, 317 (1996).
- [32] H. Baer, A. Bartl, D. Karatas, W. Majerotto and X. Tata, Int. J. Mod. Phys. A4, 4111 (1989).
- [33] D. Amidei and C. Brock, "Report of the TeV2000 Study Group on Future ElectroWeak Physics at the Tevatron", 1995.
- [34] A.D. Martin, R.G. Roberts and W.J. Stirling, Phys. Lett. B354, 155(1995).
- [35] H. L. Lai, J. Botts, J. Huston, J. G. Morfin, J. F. Owens, J. W. Qiu, W. K. Tung and H. Weerts, Phys. Rev. D51, 4763 (1995).
- [36] M. Hosch, private communication. The Wjj background was evaluated using the VECBOS monte carlo program, (see F. A. Berends, H. Kuijf, B. Tansk and W. T. Giele, Nucl. Phys. B357, 32 (1991)) while the $Wb\bar{b}$ and $t\bar{t}$ backgrounds were evaluated using the ONETOP monte carlo (see E. Malkawi and C.-P. Yuan, Phys. Rev. D50, 4462 (1994); D. O. Carlson and C.-P. Yuan, Phys. Lett. B306, 386 (1993).)
- [37] B. Mele, hep-ph/9705379.

Figure Captions

Fig. 1 The value of $\lambda''_{212}\lambda''_{332}$ versus strange-squark mass for $cd \rightarrow \tilde{s} \rightarrow tb$ to be observable at 95% confidence level. The region above each curve is the corresponding observable region. The solid curve is for the LHC, the dotted curve is for the upgraded Tevatron and the dashed line is the perturbative unitarity bound [4,5].

Fig. 2 The value of $\lambda''_{212}\lambda''_{332}$ versus the ratio $\Gamma_{\tilde{s}}/M_{\tilde{s}}$ for $cd \rightarrow \tilde{s} \rightarrow tb$ to be observable at 95% confidence level. The region above each curve is the corresponding observable region. The solid curve is for the LHC and the dashed curve is for the upgraded Tevatron.

Fig. 3 The value of $\lambda''_{212}\lambda''_{331}$ versus down-squark mass for $cs \rightarrow \tilde{d} \rightarrow tb$ to be observable at 95% confidence level. The region above each curve is the corresponding observable region. The solid curve is for the LHC, the dotted curve is for the upgraded Tevatron and the dashed line is the perturbative unitarity bound [4,5].

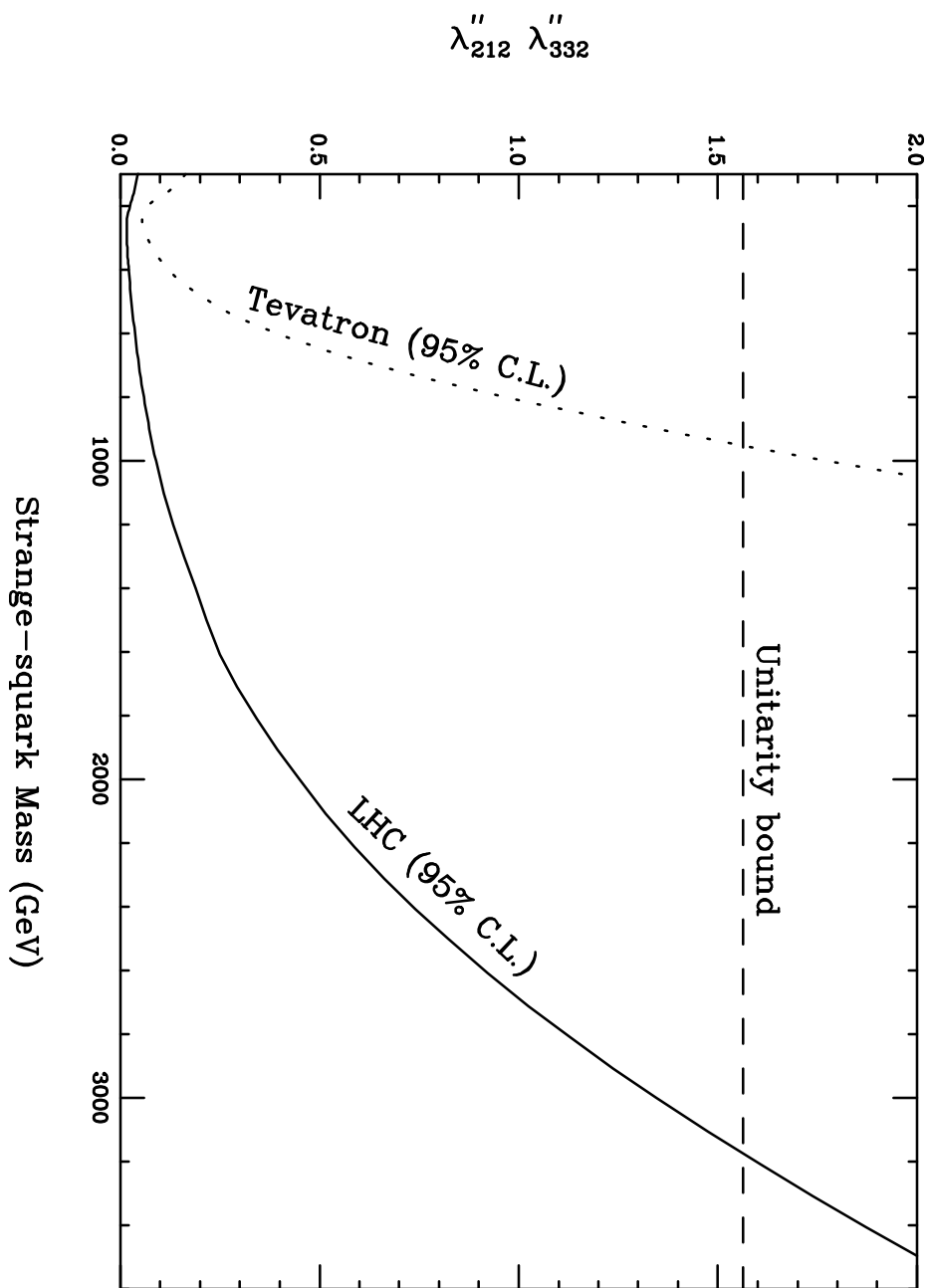
Fig. 4 The value of $\lambda'_{111}\lambda'_{133} + \lambda'_{211}\lambda'_{233} + \lambda'_{311}\lambda'_{333}$ versus the slepton mass for $u\bar{d} \rightarrow \tilde{l} \rightarrow t\bar{b}$ to be observable at 95% confidence level. The region above each curve is the corresponding observable region. The solid curve is for the LHC, the dotted curve is for the upgraded Tevatron and the dashed line is the present bound, Eqs.(25-28).

Table 1:

Signal and background cross sections in units of fb after various cuts at the Tevatron and the LHC. The $qq' \rightarrow \tilde{q} \rightarrow tb$ results have been calculated using the unitarity bound for the relevant couplings and assuming $M_{\tilde{q}} = 500$ GeV and $\Gamma_{\tilde{q}} = M_{\tilde{q}}/5$. The $q\bar{q}' \rightarrow \tilde{l} \rightarrow t\bar{b}$ results have been calculated using the present upper bound Eqs.(25)-(28) for the relevant couplings and slepton mass of 300 GeV. The slepton width is calculated by assuming $M_2 = -\mu = 250$ GeV and $\tan\beta = 2$. The charge conjugate channels are included.

Tevatron	basic cuts	basic+m(bW) cuts	basic+m(bW)+bb-tag
$cd \rightarrow \tilde{s} \rightarrow tb$	1545	1436	359
$cs \rightarrow \tilde{d} \rightarrow tb$	186	174	44
$u\bar{d} \rightarrow \tilde{l} \rightarrow t\bar{b}$	75	73	18
$q\bar{q}' \rightarrow tb$	78	75	19
$gq \rightarrow q'tb$	4	3.4	0.85
$qb \rightarrow q't$	236	224	0.45
Wbb	264	122	30
Wjj	62900	45000	0.7
$t\bar{t}$	16	7	1.8
LHC	basic cuts	basic+m(bW) cuts	basic+m(bW)+bb-tag
$cd \rightarrow \tilde{s} \rightarrow tb$	335600	304800	76200
$cs \rightarrow \tilde{d} \rightarrow tb$	125200	113600	28400
$u\bar{d} \rightarrow \tilde{l} \rightarrow t\bar{b}$	482	480	120
$q\bar{q}' \rightarrow tb$	573	547	137
$gq \rightarrow q'tb$	1104	810	203
$qb \rightarrow q't$	14150	13440	27
Wbb	756	338	85
Wjj	623600	379000	6
$t\bar{t}$	1840	644	161

Fig. 1



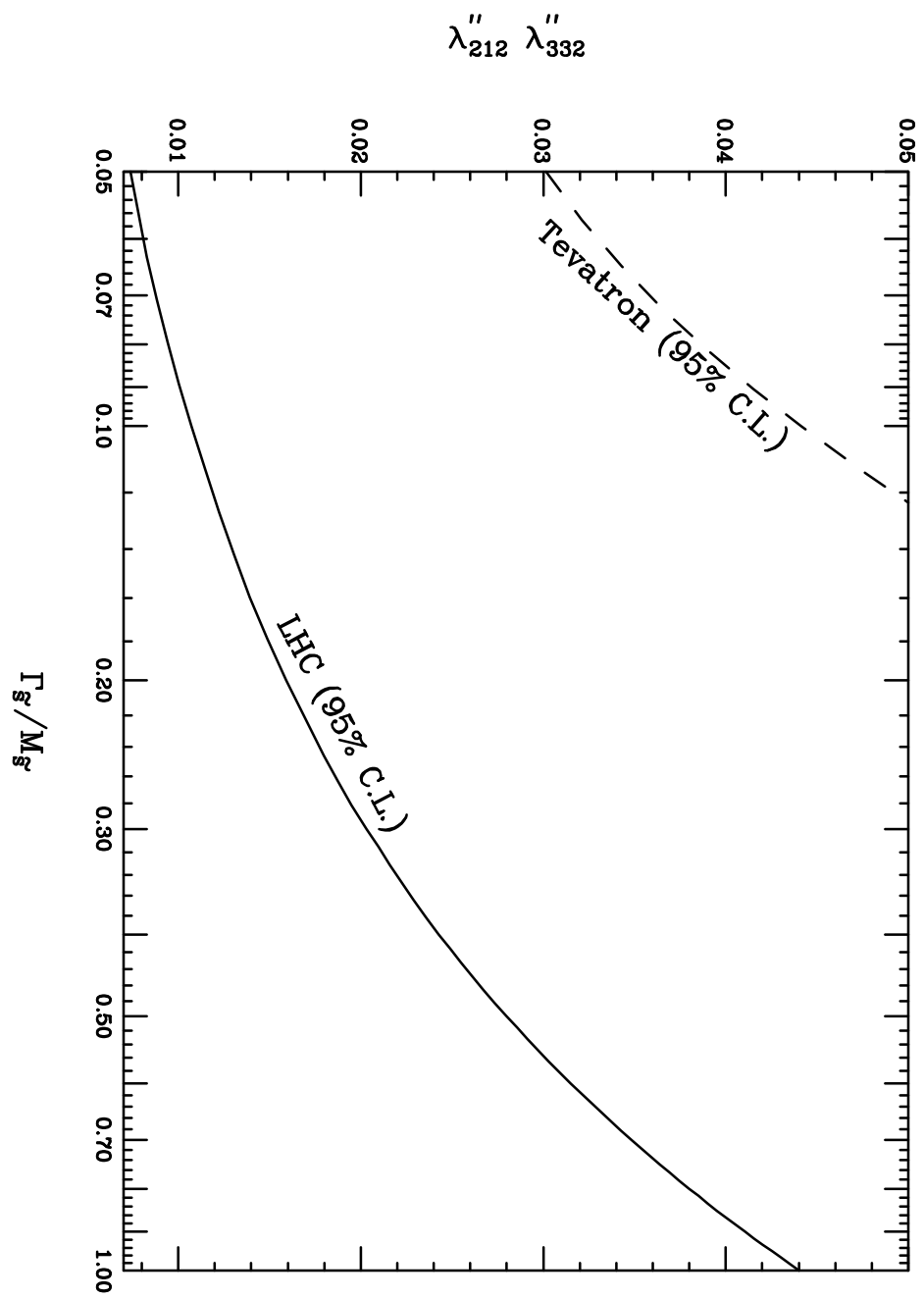


Fig. 2

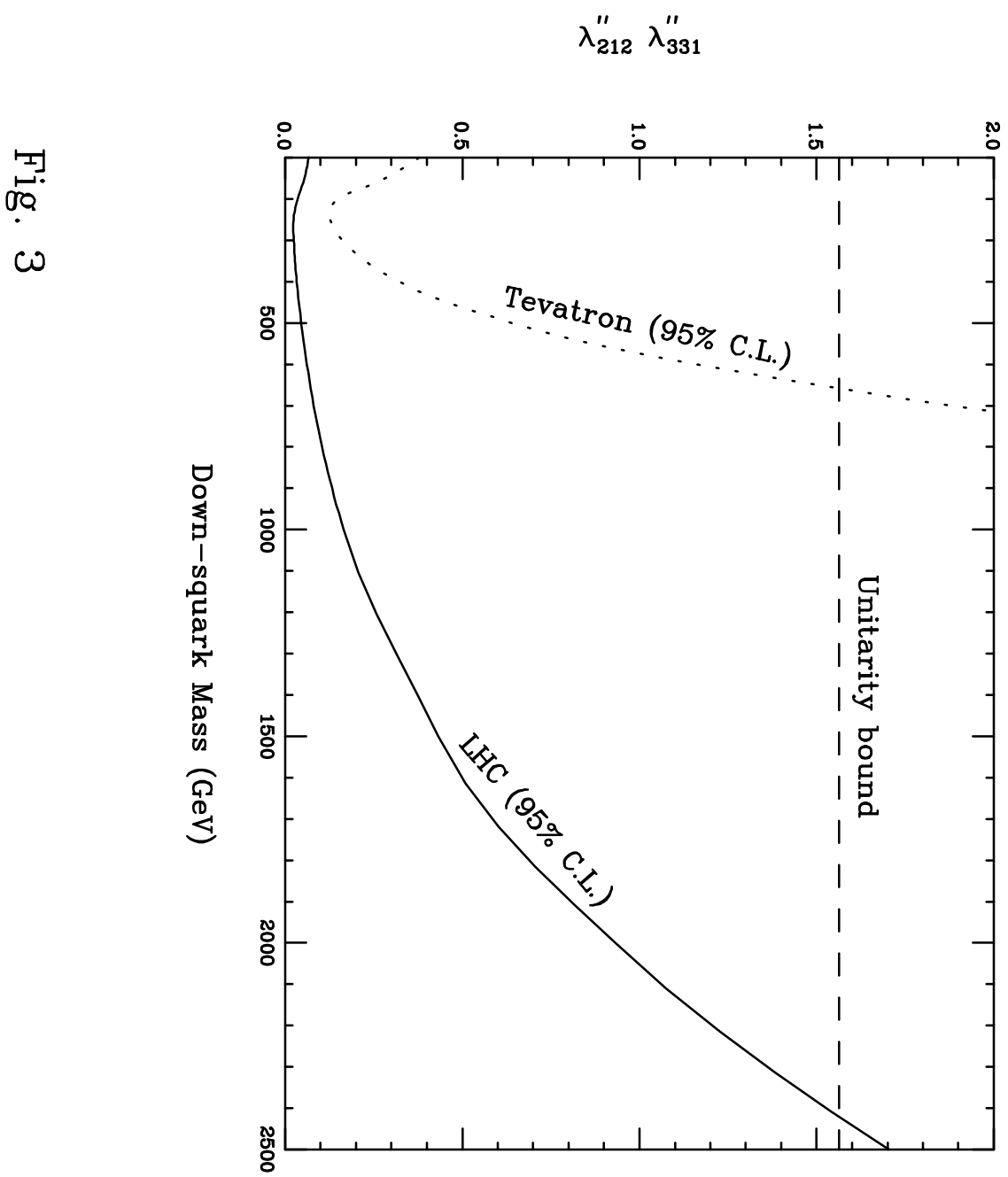


Fig. 3

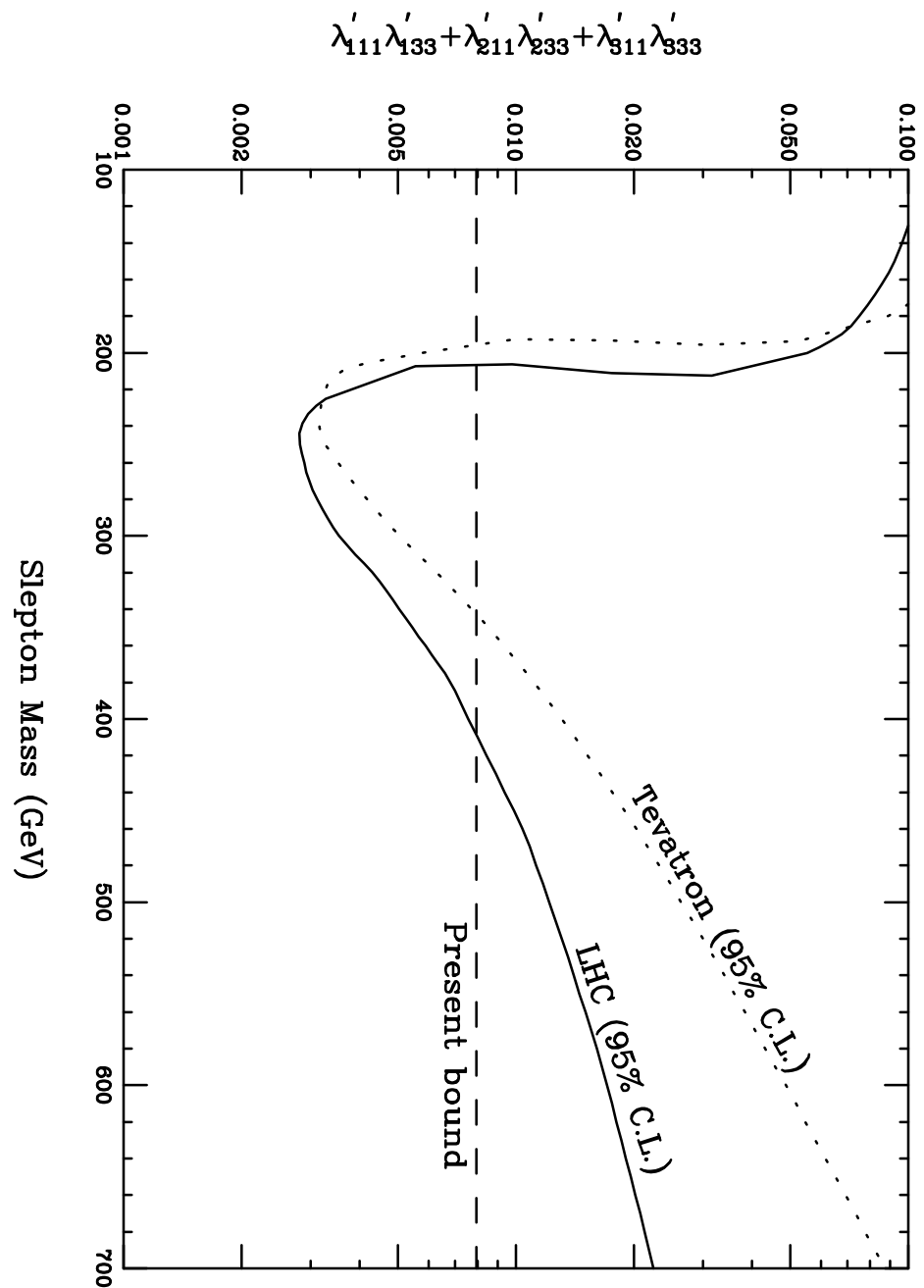


Fig. 4